SCHOOL OF ENGINEERING

Controlling the timbre of wind instruments with active impedance control

Student Name	Student Number
Eduardo José González Coll	342295

Présenté le 10.06.2022
à la Faculté des Electrical and Electronics Engineering
laboratoire LTS2
Semester Master Project
École Polytechnique Fédérale de Lausanne

pour l'obtention du grade de Bachelor's Degree in Telecommunication Technologies and Services Engineering

Hervé Lissek, Responsible Professor
Maxime Volery, Assistant Supervisor

Lausanne, EPFL, 2022

Preface

A wind instrument can generally be assimilated to a axisymmetric hollow duct, with varying (or constant) cross-section along the main axis. One extremity of the duct may be open or closed (the mouth, that can be a reed - see a saxophone -, a mouthpiece - see a trombone - or an open hole - see the flute), whereas the other end (the bell) is generally horn-shaped.
It is well known that the timbre of the instrument is associated with the shape of the bell, the type of flow excitation by the lips at the mouthpiece, and, more importantly, to the boundary conditions at the two extremities (open/open, closed/open): this specifies the nature of resonances inside the main duct, which yields a certain series of resonance frequencies (harmonics).
Then, it is noticeable that the wind families (brass, wood, etc.) are not referring to the material in which it is made, but rather on the way sound resonates inside the instrument, and a woodwind instrument might be made of brass (see the saxophone for example).
A way to alter the timbre of a cylindrical duct would be to change the acoustic impedance at the bell. For that, the concept of Electroacoustic Resonator, developed in the lab, is likely to allow real-time modification of acoustic impedance at a certain position along the duct.
This project aims at developing a scaled prototype of an active wind instrument, made of an archetypal cylindrical hollow duct with straight terminations, around which a ring of active electroacoustic absorbers will be designed to control the acoustic impedance and alter the timbre of the duct. The work will consist in:

- perform FEM simulations of the proposed design and identify potential control settings
- develop an experimental prototype of wind-instrument "scale model"
- perform acoustic assessment of the electroacoustic resonators as well as of the whole "wind instrument"

Contents

Nomenclature

Here it lays some concepts to be used throughout this project. Consider symbols as fixed values that will have the same value throughout the project. Even though some symbol values depend on temperature, their difference is neglected.

Symbols

Symbol	Definition	Value	Unit
C_{air}	Speed of sound in the air	343	[m/s]
ρ_{air}	Air Density	1.18	$[kg/m^3]$

Variables

Symbol	Definition	Unit
f	Frequency	[Hz]
M_{ms}	Moving Mass of the speaker	[kg]
R_{ms}	Mechanical Resistance of the speaker	[kg/s]
C_{ms}	Suspension Compliance of the speaker	$[s^2/kg]$
Q_{ms}	Quality Factor of the speaker	N/A
Bl	Force Factor	[Tm]
$F = Bl/S_d$	Pressure Factor	$[kg/(m \cdot s^2 \cdot A)]$
Z	Impedance	$[kg/(m^2 \cdot s)]$
R_{st}	Target Mechanical Resistance	[Pa*s/m]
Q_t	Target Quality Factor	N/A
f_t	Target Resonance Frequency	[Hz]
S_d	Effective Piston Area	$[m^2]$

1 Theory

A *wind instrument* is a musical instrument that incorporates some resonator (usually a tube) in which the reed (or the player's lips) sets a column of air into vibration. Both the bore of the instrument and the player's vocal tract behave nearly linearly, while the reed (or the player's lips) behave in a non-linear way.[1] The scope of this project does not reach further than the linear behaviour of the instrument. The bore resonances, near which instruments usually operate, have high impedance. When the acoustic wavelength is large compared to the cross-section dimensions of the bore, it is usual to consider one-dimensional models where acoustics is described in terms of flow rate and pressure.

1.1 Input Impedance

Input impedance is the impedance of the instrument at the beginning of the duct. In acoustics, *impedance* is defined as a function of frequency, whose input signals are linearly related like a ratio between pressure and particle velocity at a given point. Assuming that plane waves can propagate inside the duct in 1D as:

$$\nabla^2 p - \frac{1}{c^2}\frac{\partial^2 p}{\partial t^2} = 0 \rightarrow \frac{\partial^2 p}{\partial x^2} - - \frac{1}{c^2}\frac{\partial^2 p}{\partial t^2} = 0 \tag{1.1}$$

The input impedance, when normalized with the air impedance, reads as:

$$Z_{air} = \rho_{air} c_{air} \rightarrow Z_{in}(w) = \frac{p(w)}{Z_{air} v(w)} \tag{1.2}$$

Although the characteristic impedance of the medium depends on the density of the air ρ, the speed of sound c_{air}, and the cross-section area at the pipe's input, it is going to be considered a fixed value Z_{air} in the scope of this project.

1.2 Output Impedance

At the end of the duct, the radiation is modelled by the dimensionless radiation impedance Z_r given by Silva [4] as a fraction of two polynomials. A vital feature of wind instrument bores is the existence of weakly damped resonances.

1.2.1 Terminal Impedance

Every duct can have different types of termination. However, the first simulations are going to be simulated with three terminations: open, closed and soft. This can be considered as part of the boundary conditions. Depending on the type of terminal, the behaviour of the tube will change. Once the three terminations are considered, it can be concluded the kind of absorber it is needed. In this case, the magnitude of the impedance must be low since the radiation impedance is also low in magnitude.

Closed Termination

It is considered closed termination when the boundary conditions impose $q_{out} = 0$ (null output flow velocity). At low frequencies, it translates as a compression effect of the air, where V is the volume of the duct. The general formula (1.3) describes as:

$$q_{in} - q_{out} = jwp\frac{V}{\rho_0 c_0^2} \tag{1.3}$$

$$Z_{in} = Z_{air}\tanh(-jkL + \operatorname{arctanh}\left(\frac{Z_{out}(L)}{Z_{air}}\right)[11] \tag{1.4}$$

It can be understood as an infinite impedance where $Z_{out} \to \infty$. [10]

Open Termination

It is considered open termination when the boundary conditions read (in a 1^{st} order approximation) $p_{out} = 0$ (null pressure at the output). At low frequencies, it translates as the inertia effect of the air in the tube. It is considered low frequency when the wavelength is much bigger than the duct length. The flow velocity is constant within the duct and it exists a pressure drop between the input and the output. The general formula (1.5) describes as:

$$p_{in} - p_{out} = jw\frac{\rho_o L}{S}q_{in} \tag{1.5}$$

It can be understood as a null impedance where $Z_{out} = 0$.

Anechoic Termination

Anechoic terminations are assemblies connected to duct end functioning to transform a duct of finite length into an acoustically infinite long duct to provide a non-reflecting termination for many in-duct aero-acoustic measurements. [13]

1.3 Electroacoustic Absorbers

In order to change the timbre of the instrument, it is needed to change the impedance in the duct. There are different methods to succeed in this endeavour:

- **Passive absorbers**: a passive absorber is either based on porous material (e.g. rockwool), which is broadband but bulky (size > $\lambda/4$), or based on a resonant structure such as Helmholtz, bass-trap or a passive speaker (e.g. unconnected), but because of the resonant nature is band limited.
- **Active absorbers**: consist in varying the impedance of a part of the enclosure boundaries through a transducer to balance the sound field thanks to the absorbed sound power into the boundary elements. This report defines an active absorber based on the model inversion of the speaker: measuring the pressure in front of the speaker, and knowing the model of the speaker, one can calculate what is the required current to inject in the coil such that the desired velocity (target impedance) is achieved by the membrane.

Turning an electrodynamic loudspeaker into an electroacoustic absorber enables the sound power of incident waves to be controlled. To achieve maximal sound absorption under normal incidence, the specific acoustic impedance $Z_s(s)$ should be set to a target-specific acoustic resistance R_{st} equal to the characteristic specific acoustic impedance of the medium $Z_c = \rho c$.

This condition implies that the phase between the total sound pressure $P_t(s)$ at the diaphragm and diaphragm velocity $V(s)$ should be negligible over the whole frequency range.
However, reactive terms such as compliance and mass induce a mismatch away from the resonance frequency. Thus, they cannot be cancelled entirely. The sound pressure at x= L (if the source is in x= 0) is satisfied by the solution of the Helmholtz equation (1.6):

$$P_{tx}(w) = A(w)\left(e^{-j\Gamma x} + R_L(w)e^{j\Gamma(x-2L)}\right) \tag{1.6}$$

Where A is the incident amplitude, R_L the reflection coefficient and Γ is explained in equation (2.1).

1.4 Analytical study of the 1D case

In order to have an idea of what to expect in later simulations, an analytical calculation of the input impedance is done with and without absorbers. For a Matlab implementation, the output impedance needs to be computed. The equation that satisfies the radiation impedance Z_r is:

$$Z_r = 1 - [\frac{J_1(2ka)}{(ka))}] + S_1(\frac{2ka}{ka}) \tag{1.7}$$

where the J_1 is the Bessel function of the first kind of order one and S_1 is the Struve function of the first order. [7] [8]

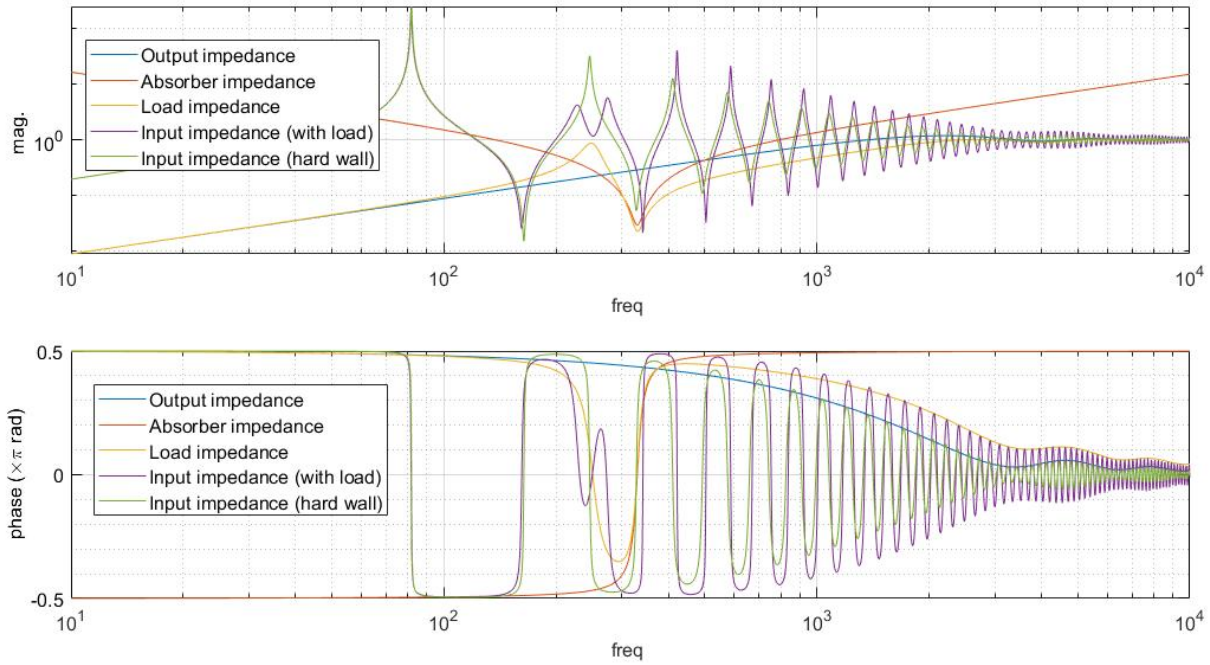

Figure 1.1: 1D analytical study Matlab

Figure (1.1) shows the analytical result of the impedances that are going to be simulated afterwards. In green is shown the input impedance of the duct with no absorber (termination is the radiation impedance, displayed in blue). In purple is the input impedance with a 1-degree-of-freedom resonant absorber at the termination (which impedance is seen in red). The termination impedance of the purple case is the parallel of the radiation and absorber impedances, shown in yellow.
To modify the input impedance (and thus the resonances), the absorber impedance must be of similar or lower magnitude as the radiation impedance at the frequency range of interest because both impedances are in parallel, and the lower magnitude will prevail.
This analytical study summarises what is expected to see during the simulations and later in the measurements.

2 Finite Element Method

The Finite Element Method (FEM) design uses COMSOL Multiphysics ® to simulate the electroacoustic absorber. As to the instrument design, it is considered a cylindrical duct to be a sufficient representation of the bore for configuration simplicity. In particular, the study will only be interested in the input and output impedance behaviour, especially when working with low and mid frequencies.
In this simulation, air damping is assumed as an attenuation coefficient modelling the viscothermal losses in a cylindrical duct, defined in the constant propagation [6] by the equation:

$$\Gamma = j\frac{w}{c} + (1+j)3.10^{-}5\frac{\sqrt{f}}{R} \tag{2.1}$$

It is often ignored the effect of dispersion, replacing $(1 + j)$ by 1 in the equation (2.1). The simulations can be divided into three main terminations depending on which absorbers they have: Hardwall, Passive and Active. Each of them can then be subdivided into three different types of termination: closed, open and anechoic.

- Electroacoustic Absorbers
  - Hardwall Absorber
    - Closed Termination
    - Open Termination
    - Anechoic Termination
  - Passive Absorber
    - Closed Termination
    - Open Termination
    - Anechoic Termination
  - Active Absorber
    - Closed Termination
    - Open Termination
    - Anechoic Termination

This project focuses on the active control of the impedance in open termination, forcing the output pressure to be null. However, for a better understanding of the behaviour of the input impedance inside the duct, the first simulation will be a hardwall absorber, i.e. no absorber and all of its terminations. The hardwall simulation will establish the reference to compare the contrast between the different terminations. All the graphs showing the input impedance have been normalized by the air impedance Z_{air}.

2.1 Design of 2D active absorption model

The first design is a 2D axisymmetric model. It is beneficial for efficiency computing reasons. The geometry is a revolved rectangle with an input impedance of 1[Pa] and an ideal continuous absorbing impedance at a parametric distance from the end of the impedance tube. In Figure (2.1), at z=-0.85[m], it is assigned a pressure source of 1[Pa]. At z=0.85[m] there are going to be different terminations.

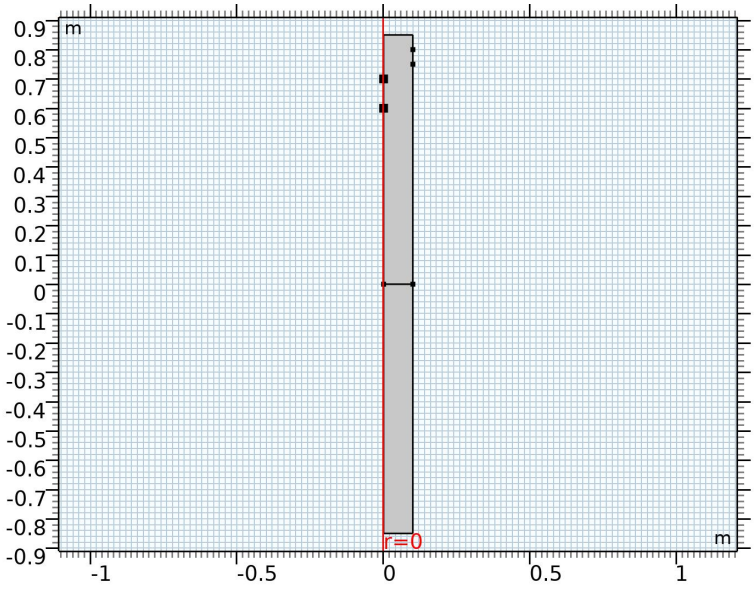

Figure 2.1: 2D Geometry

For the analysis in the frequency domain, it is required to know the speaker's characteristics. A classical method for parametrization of the impedance is based upon identifying the resonances in terms of angular frequencies and quality factors of the speaker.
The specific impedance of the speaker can be defined as:

$$Z_s(s) = \frac{sM_{ms} + R_{ms} + \frac{1}{sC_{ms}}}{S_d} = \frac{s^2 + \frac{sw}{Q_{ms}} + w^2}{\frac{sw}{Q_{ms}}} R_s \tag{2.2}$$

where

$$C_{ms} = \frac{1}{w^2 M_s} \tag{2.3}$$

$$S_d = 2\pi ad \tag{2.4}$$

$$R_{ms} = \frac{1}{wQ_{ms}C_{ms}} \tag{2.5}$$

Where in equation (2.4) $a = 0.1[m]$ is the radius of the circular piston, S_d is the effective piston area and $d = a/2 = 0.05[cm]$. Terminal impedance plays a significant role in the behaviour of the duct. Depending on the termination, the input impedance may behave differently, thus, changing the timbre of the duct.

The following simulations will show the behaviour of all the states of the absorbers with every possible termination.

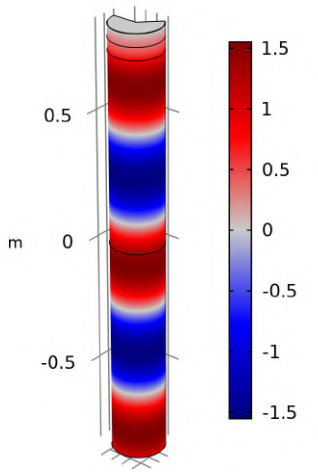

Figure 2.2: Acoustic pressure level computed at 490 Hz in the waveguide terminated by the electroacoustic absorber ring.

This geometry at Figure (2.2) can be seen when the Figure (2.1) is revolved. Here it is shown a closed termination at the top, representing a hardwall, while in the bottom there is a pressure source of 1[Pa]. Color red represents the highest values of pressure, whereas color blue represent the lowest values.

2.1.1 Simulations

The following simulations are done with the geometrical values of the section 2.1.

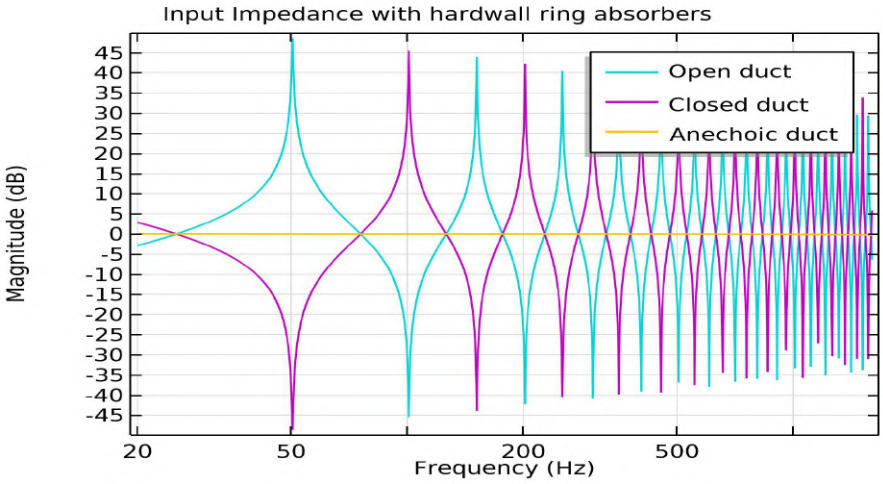

Figure 2.3: Input Impedance without absorbers

In the first one is shown a duct with no active nor passive control. There are no absorbers. Thus, the ring is a continued Sound Hard Boundary. In this simulation, there are three-terminal impedances: Open, Closed and Anechoic. (Figure 2.3.)
The next simulation (Figure 2.4) considers the electroacoustic absorber ring with a passive behaviour. The passive ring is modelled by the equations $C_{ms} = 6.9493e-4[s^2/k]$ (2.3), $R_{ms} = 0.2659[kg/s]$ (2.5), $S_d = 0.031416m^2$ (2.4), $Q_{ms} = 3.19$ and $M_{ms} = 0.5[g]$.

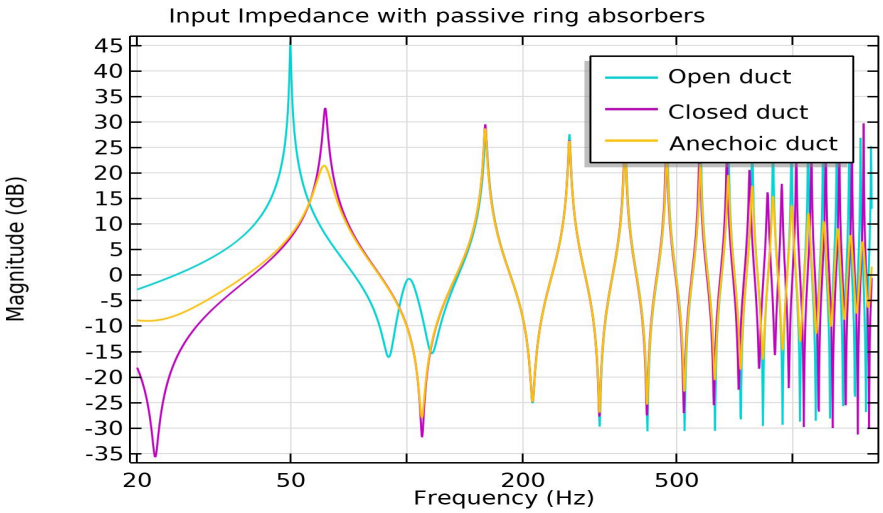

Figure 2.4: Impedance in the duct passive ring of absorbers

For the representation, the y-axis shows the input impedance as $20log_{10}(\frac{Z_{in}}{Z_{air}})$ over the frequency. In Figure (2.4) it is shown that with a passive ring of controllers, the magnitude of the input impedance is higher when the duct has an open termination.

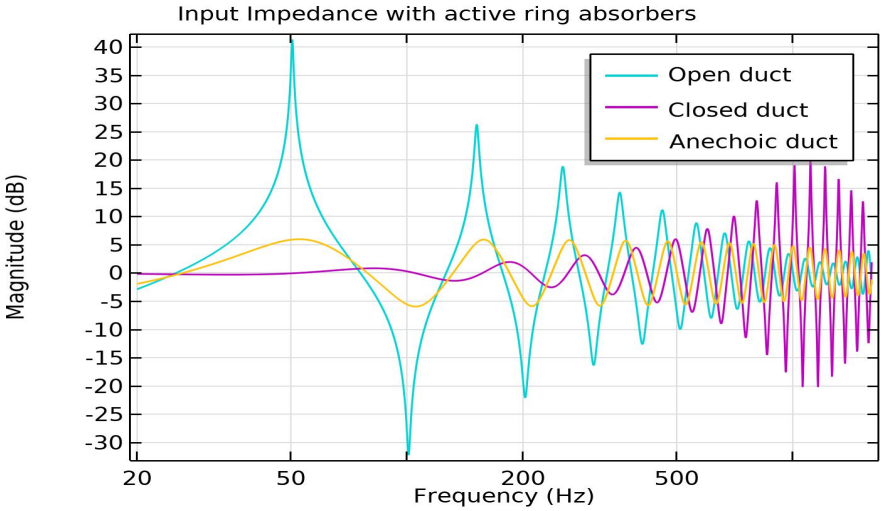

Figure 2.5: Input Impedance with active ring absorbers

The simulation in Figure (2.5) uses an active control over the electroacoustic ring absorber. When the ring behaves as an active absorber the resistance is changed, i.e., to adapt it to the impedance of the air, so that $R_{ms} = 12.715[kg/s] = S_d Z_{air}$. For the active simulations, the only value changed is R_{ms}, keeping the same values for the other Thiele/Small parameters.

It is shown that when the termination is an open duct, the higher the frequency, the more effect the absorber has over the magnitude. Higher frequencies also break the assumption of considering the absorber at the same position as the termination, due to the small size of the wavelengths. The opposite happens when the termination is a closed duct, where at high frequencies, the magnitude of the impedance grows.

Anyhow, an open termination with the three different ring states is closer to what will happen in reality. (Figure 2.6)

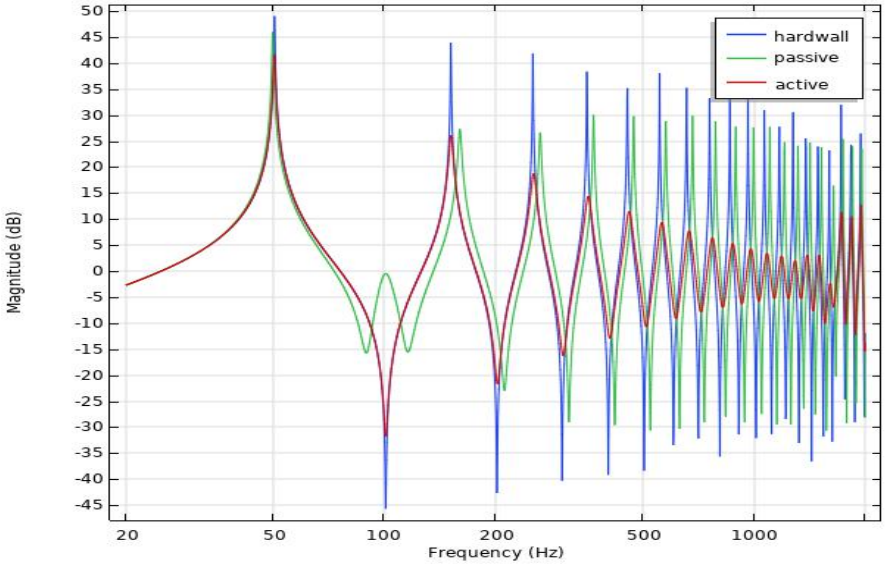

Figure 2.6: Input Impedance with an open duct termination.

This last simulation in Figure (2.6) is the overview of the open ducts of the three previous simulations. Thus, when the termination is an open duct, a ring of active absorbers can control the impedance starting at the second resonance peak.

2.2 Design of 3D active absorption model

2.2.1 Geometry

After a successful simulation in an open duct, where the input impedance lowers its value with active control starting at the second resonance peak, the following will be a 3D active control model.

The geometry is a cylinder representing the duct. The absorbers are presented as a 2D circle plane for simplicity.

In this model, there are four speakers, as in the real model, there will be four electroacoustic absorbers. (Figure 2.7)

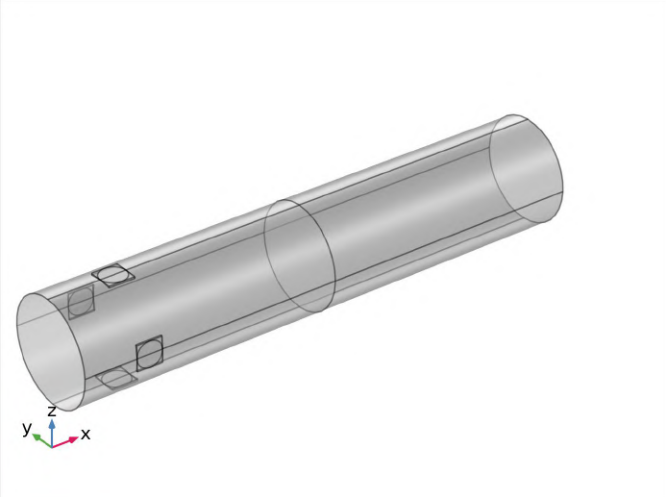

Figure 2.7: 3D Geometry with 2D absorbers

The simulation has been done with the same values as before, with a resonance frequency of 270 Hz, a quality factor of $Q_{ms} = 3.19$, the passive impedance with a R_{ms} (equation: 2.5). When there is active control, $R_{ms} = S_d Z_{air}$, keeping the other parameters as before.

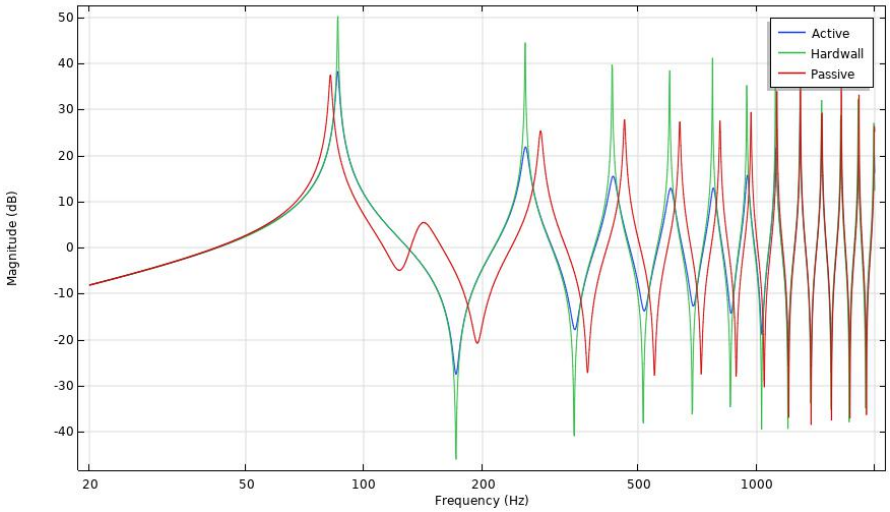

Figure 2.8: Input impedance with 3D Geometry and 2D absorbers

The results of the simulation in Figure (2.8) show a slightly reduction of the the magnitude of the impedance in the first peak, and over 20dB's of reduction compared to the hardwall in the second peak when active control is used.

The following and last simulation done represents the physical model prototype. The geometry of this simulation consists of a rectangle with four electroacoustic absorbers. The absorbers are still 2D circles. It can be noticed that the geometry is just 1/8th of the actual volume. This is because the geometry presents symmetry. Thus, this geometry saves computing time.

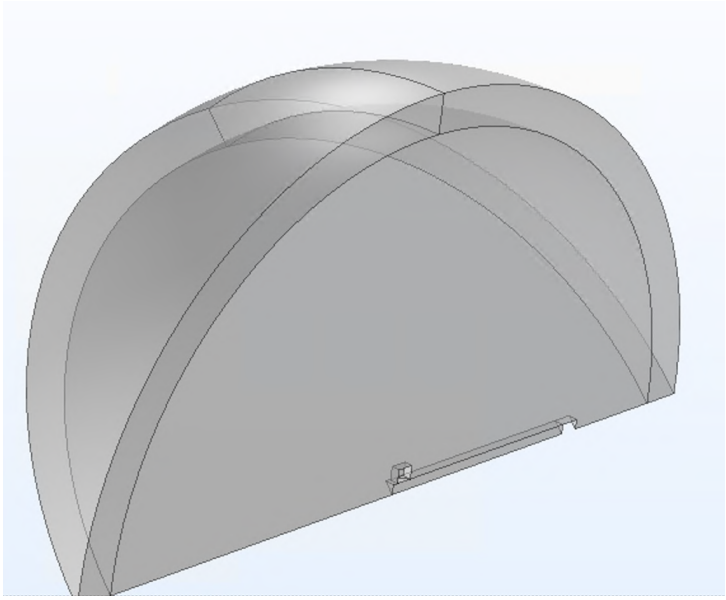

Figure 2.9: 3D Geometry

However, in this simulation it is considered the surrounding exterior space. The following step is to consider the pressure that the speaker produces outside to prevent possible interference between it and the radiation impedance. For this purpose, it is imperative to define some boxes covering the absorber.

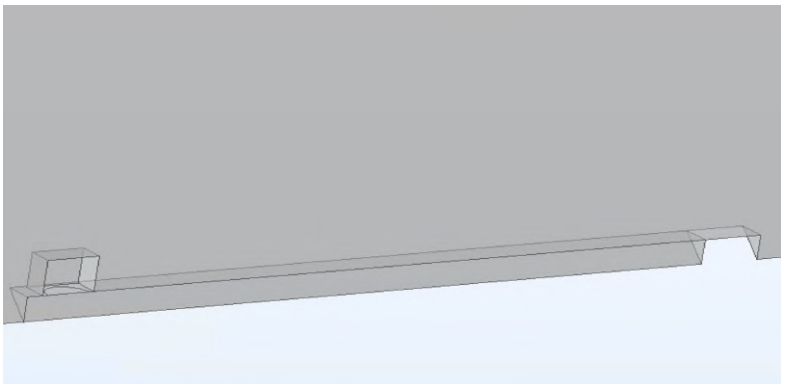

Figure 2.10: 3D Geometry Duct

Covering the absorber with a box will help cancel unwanted pressure outside. On the other hand, this will add stiffness to the absorber. It could be measured precisely the volume of the speaker, cables, and screws inside the box to have a more realistic result of what to expect on a measurement on the physical prototype.

Moreover, in this geometry, it is considered that the microphone controlling the absorbers is located in the middle of the duct in the centre between all the speakers. In Figure (2.10), this position would correspond to the position below the speaker. In this project, the box has a volume of 0.5677 [L]. The volume of the mounted speaker is approximately 0.2 [L]. The difference between both of them would be roughly 0.3[L]. Adding an enclosure with a smaller volume than the equivalent speaker volume produces an increase in stiffness.

In this simulation, the impedance Z_{st} is targeted with the transfer function [2]:

$$\theta(s) = \frac{1 - \frac{Zss}{Zst}}{F} = \frac{I(s)}{P_t(s)} = \frac{S_d Z_{st}(s) - Z_m(s)}{Bl Z_{st}(s)} \tag{2.6}$$

The absorber is controlled by the membrane normal velocity:

$$v = \frac{P_t(s) - F * I(s)}{Zss} \tag{2.7}$$

Here, $F = Bl/S_d$ represents the pressure factor, which in the simulation will have a value of $F = 953.13[kg/(ms^2 A)]$ and Z_{ss} the speaker passive specific impedance and $I(s)$ the control for the electrical current.
Figure (2.11) shows the block diagram of the controlled loudspeaker by measuring the total sound pressure at the diaphragm. The controller in the image is modelled by the equation (2.6). In the image, the electrical impedance is absent from the control. [2]

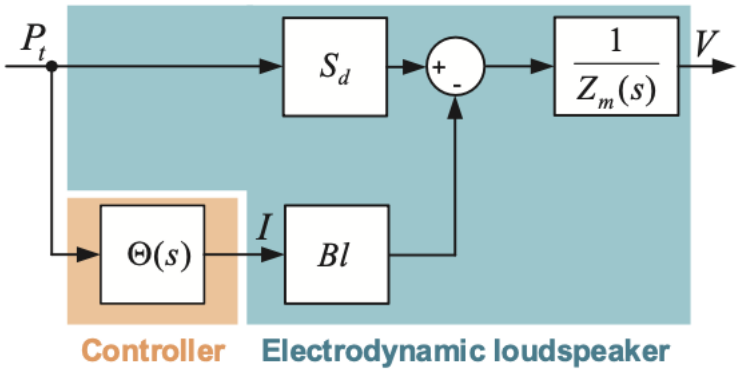

Figure 2.11: Etienne Thierry Jean-Luc. Room modal equalisation with electroacoustic absorbers. EPFL, 2016.

In the simulation of this geometry, elaborated in subsection (2.2.2), the natural values of the speaker (see Table 2.1) are used in the measurements. The active control is regulated by changing the quality factor, the mechanical resistance and the resonance frequency.

2.2.2 Simulation

The values used in order to target the second resonance in the duct are $R_{st} = 50[Pa * s/m]$, $Q_t = 11$ and $fs = 250[Hz]$. For this simulation, the natural values of the speaker are used in the measurements, which are shown in table (2.1) below.

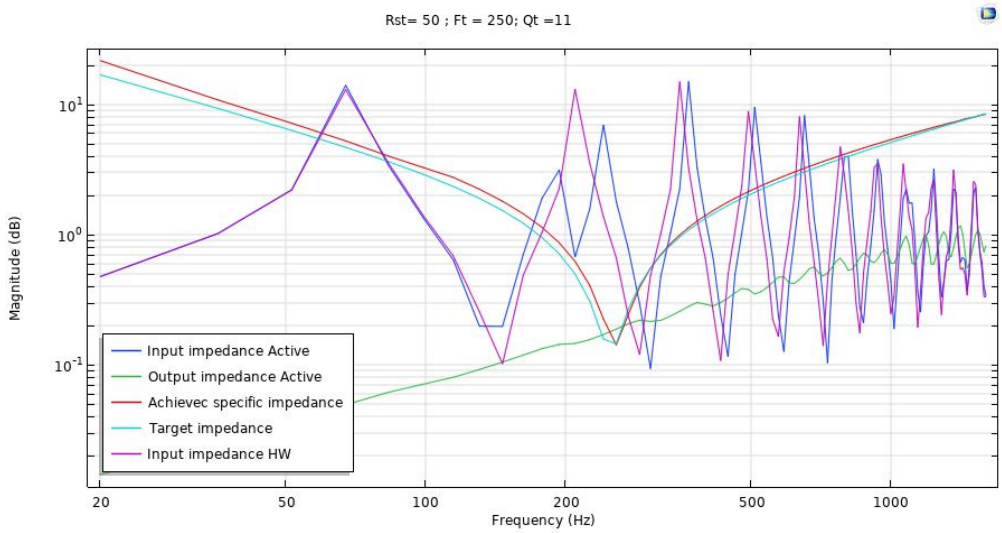

Figure 2.12: 3D Magnitude COMSOL

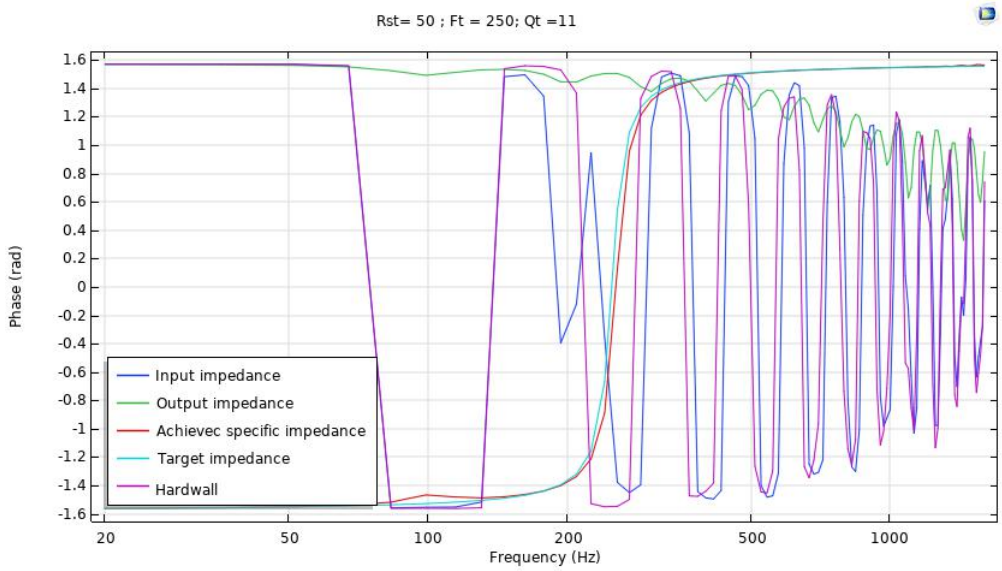

Figure 2.13: 3D Phase COMSOL

SPX-30M

Symbol	Definition	Value	Unit
Z	Impedance	8	[Ω]
fs	Resonance Frequency	100	[Hz]
M_{ms}	Moving Mass	2.1	[g]
R_{ms}	Mechanical Resistance	0.38212	[kg/s]
C_{ms}	Suspension Compliance	1.23	[mm/N]
Bl	Force factor	3.05	[Tm]
Sd	Eff. cone area	32	[cm^2]
Q_{ms}	Mechanical Quality Factor	3.453	
V_{as}	Equivalent Volume	1.8	[L]

Table 2.1: SPX-30M

In order to control the parameters with the best accuracy possible, it is required to understand the behaviour of the parameters. The quality factor narrows the target frequency, being more refined and more precise when the it is higher. The lower the quality factor (the higher the damping) the higher the bandwidth.
Moreover, the mechanical resistance enhances or reduces the effect of the absorption inversely to its value.
The simulation in the Figure (2.12) shows how to target a resonance; it ought to aim at a higher frequency than the one to be reduced.
It is noticeable that the targeted impedance and achieved are slightly displaced. The explanation is that the microphone's position is not in the speaker but a little bit further. For lower frequencies, where pressure is distributed mostly uniformly, the target impedance and the achieved specific impedance are very similar. However, the higher the frequencies, the more displacement it will be. One possible solution is to put more microphones, so we have a better measurement of the pressure in different spots.
Additionally, the phase encounters a change at the same frequency as the impedance has been diminished.

3 Measurements

3.1 Physical Model

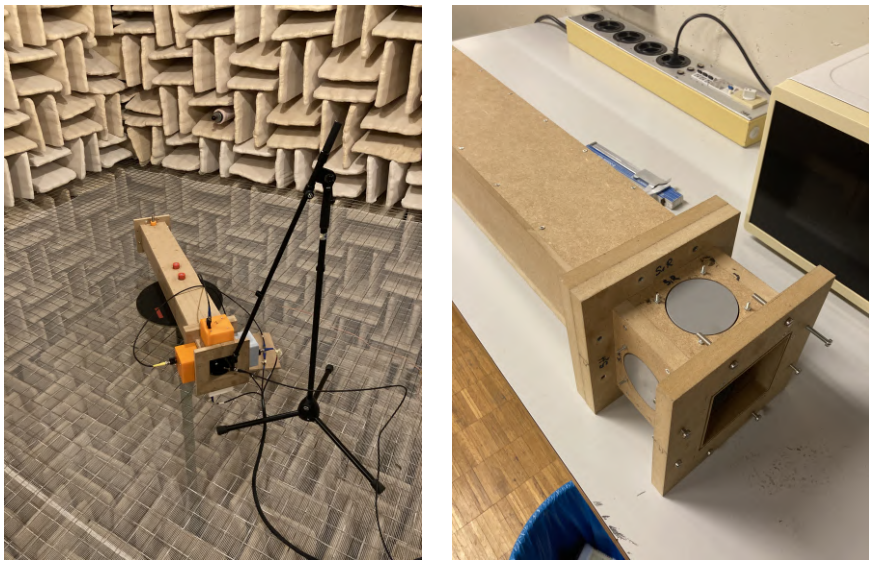

(a) Absorbing Physical Model (b) Hardwall Physical Model

Figure 3.1: Experimental prototype of wind-instrument "scale model"

In developing the scaled prototype, the chosen design was an orthotope (also called a hyper-rectangle or a box) hollow duct with straight terminations, surrounded at the end by four active electroacoustic absorbers. The design was chosen due to the convenience when installing the electroacoustic absorbers compared to an archetypal cylindrical design. This decision was sustained with the assumption of the plane waves until 1.6 kHz. [12] When waves are not plane anymore, then the transverse modes can affect the stability of the control at higher frequencies, but that goes beyond the limits of this study. For the hardwall measurements, we added some plastic lids covering the holes, as we see in Figure 3.1b. Four speakers were added in the holes for the passive and active measurements, and 3D printed five boxes to cover the speakers to prevent acoustic radiation impedance from the rear of the mounted speaker to the exterior.

3.2 Instrumentation

Material

- Five Monacor SPX-30M
- Five one-side-open boxes.
- Polytec OFV-5000 VIBROMETER CONTROLLER
- Brüel & Kjær Power amplifier
- Brüel & Kjær Type 3160-A-042 Output Generator Module 50kHz
- Speedgoat baseline real-time target machine expressly designed for Simulink Real-Time
- Microphone PCB PIEZOTRONICS Model: 378B02 SN 128220.
- Microphone model: 6974

Software

- Matlab & Simulink
- Brüel & Kjær PULSE® Lapshop acquisition system.

3.3 Measurements

3.3.1 Setup

For the characterization of the absorbers, the vibrometer had to point to the absorber with an angle of *alpha* to reach the absorber (Figure 5.3). The solution was to multiply the impedance by a correction factor of velocity. The setup in the Figure 3.3 has been simplified. Connectors, current to voltage converters, and amplifiers were used on the actual setup (Figure 5.2).
For the impedance measurements, the frequency worked with a spectrum of frequencies until 1.6kHz, because of the plane-wave behaviour, with a centre frequency of 820 Hz.
For the characterization of the input speaker, reflective tape was added to the speaker so the Polytec would perceive the velocity better. All the measurements were made with a Logarithmic Swept Sine. As for the setup of the characterization and measurement of the input impedance, the vibrometer focalized in the diaphragm of the speaker.
For this setup, two pairs of microphones were used to measure the input impedance and the transfer function between sound pressures. [10]
In order to characterize the absorbers and get their parameters, the passive behaviour of the speakers is needed. The parameters needed know are f_s, Q_{ms}, R_{ss} and the pressure factor. The first three ones can be obtained by a passive speaker measurement. A target impedance was set for the latter to retrieve the force factor (equation 2.6).

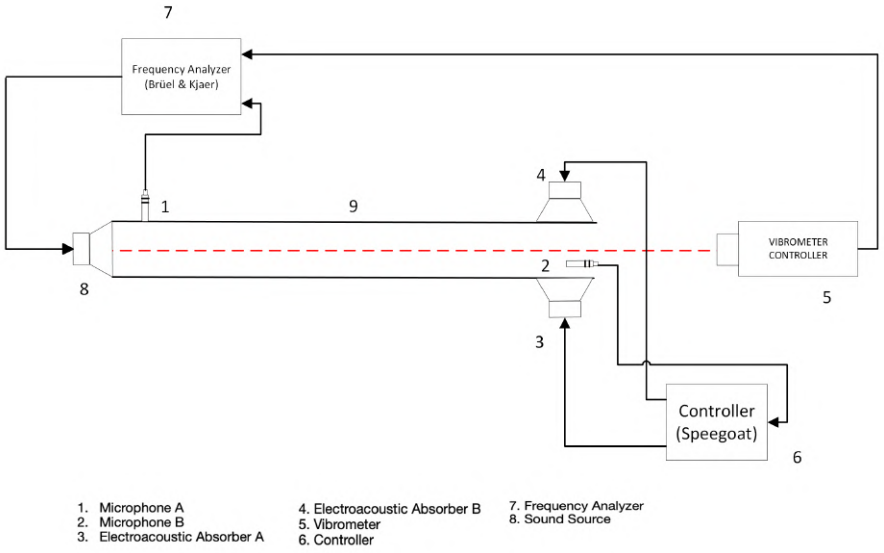

Figure 3.2: Active Control Setup

The results of the characterization of the speakers were:
Speaker 1: Fs = 196.46 [Hz]; Q_{ms} = 7.92;R_{ss} = 113.20 [Pa*s/m] ; Bl/Sd = 770.04 [Pa/A] (3.4a)
Speaker 2: Fs = 203.37 [Hz]; Q_{ms} = 4.85;R_{ss} = 181.14 [Pa*s/m]; Bl/Sd = 656.55 [Pa/A] (3.4b)
Speaker 3: Fs = 210.45 [Hz]; Q_{ms} = 4.43;R_{ss} = 208.86 [Pa*s/m]; Bl/Sd = 649.12 [Pa/A] (3.4c)
Speaker 4: Fs = 204.63 [Hz]; Q_{ms} = 5.71;R_{ss} = 175.40 [Pa*s/m]; Bl/Sd = 699.48 [Pa/A] (3.4d)

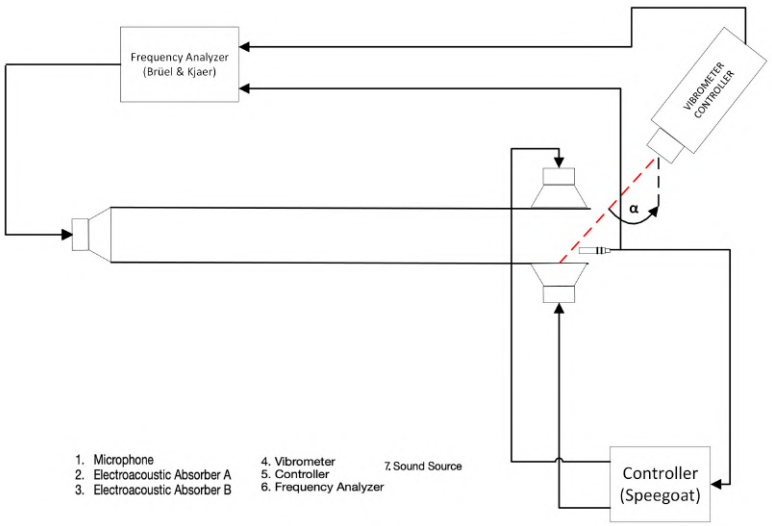

Figure 3.3: Absorbers Control Setup

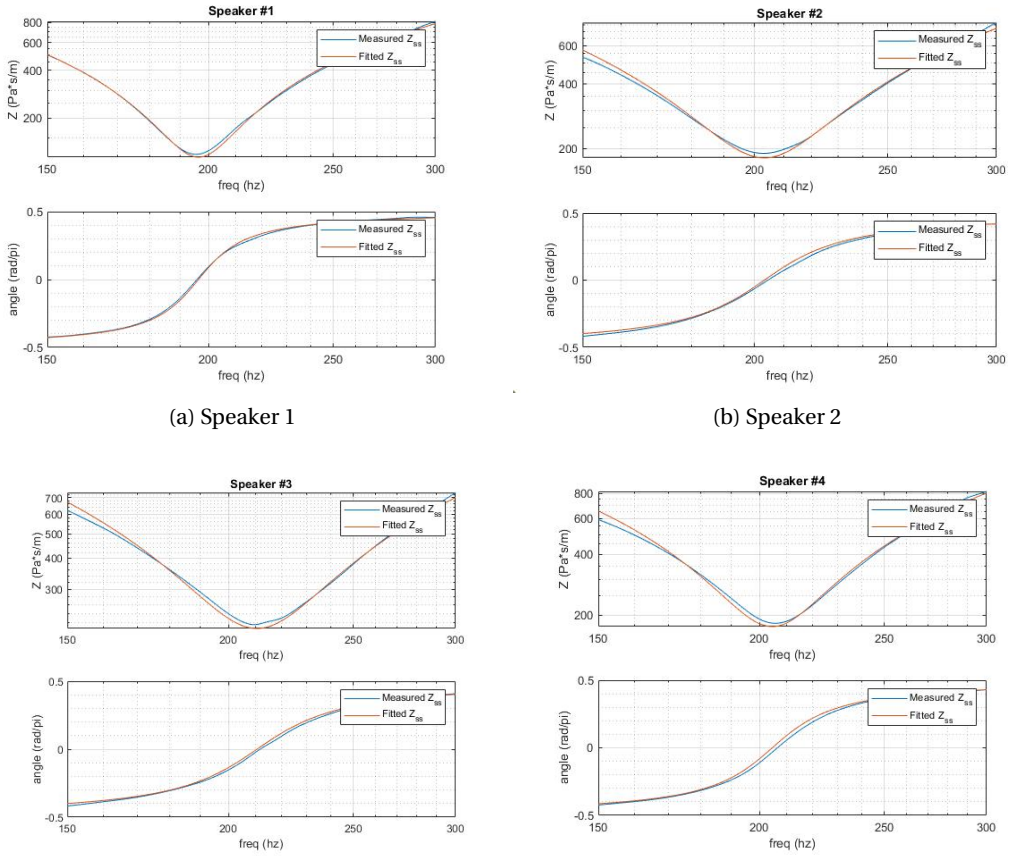

(a) Speaker 1

(b) Speaker 2

(c) Speaker 3

(d) Speaker 4

Figure 3.4: Characterization of the speakers

Figure (3.4) shows the measured impedance and fitted one for each of the speakers. A polynomial fitting was used to estimate the first three parameters of the speaker. To preserve a good quality of data, the frequency was masked between 150 [Hz] and 300 [Hz]. This range was chosen because the resonance frequency was expected to be inside this range of frequencies, and below 150 [Hz], the coherence shows non-linear behaviour.

Considering a typical regression model, where $\vec{b}$ is the response vector, A is the designed matrix and $\vec{x}$ is the parameter vector, the equation modelling this is:

$$\vec{b} = A\vec{x} + \epsilon \rightarrow \vec{b} = A\vec{x} \tag{3.1}$$

In this case, ϵ would be the error, but for simplicity, it is neglected.

In order to compute the coefficients, the equation (3.1) can be described as a system of linear equations:

$$\begin{bmatrix} \vec{R} \\ \vec{x} \end{bmatrix} = \begin{bmatrix} \vec{0} & \vec{1} & \vec{0} \\ \vec{w} & \vec{0} & \frac{\vec{-1}}{w} \end{bmatrix} \begin{bmatrix} M \\ R \\ K \end{bmatrix} \tag{3.2}$$

In the response vector of equation (3.2), $\vec{R}$ translates as the real part of the impedance, while $\vec{x}$ represents the imaginary part. Moreover, in the parameter vector, M represents the moving mass of the speaker. R represents the mechanical resistance, and K represents the stiffness, where $K = \frac{1}{C_{ms}}$.
The vector of estimated polynomial regression coefficients would be described by the equation:

$$\vec{x} = (A^T A)^{-1} A^T \vec{b} \rightarrow \vec{x} = \vec{b}/A \tag{3.3}$$

When the parameter vector is computed as equation (3.3) suggests, the parameters of the speakers can be retrieved, including the force factor. With them, the impedance equation (2.2) can be computed and plotted, as Figure (3.4) shows.

3.3.2 Brüel & Kjær PULSE® Lapshop

Brüel & KjærLapshop software is used to run the measurements. In order to supervise the proper functioning of measurements, the coherence is computed as:

$$G_{pv}(f) = \frac{|G_{pv}(f)|^2}{G_{pp}(f)G_{vv}(f)} \tag{3.4}$$

The reference signal p stands for the pressure while the signal v stands for the velocity.
$G_{pv}(f)$ is the Cross-spectral density between p and v, and $G_{pp}(f)$ and $G_{vv}(f)$ the auto spectral density of *pressure* and *velocity*, respectively. If the system is linearly ideal, the signal $G_{pv}(f)$ will be one or close to one. It is considered that the signals are not coherent when the value moves away from one.
Equation (3.4) is true for the two setups shown in Figures (3.2 & 3.3). When measuring the transfer function of the radiated pressure over the input pressure, the two signals modelling the coherence were these two pressures, as the setup in Figure (5.4) shows.

4 Results

After a measure, the data is stored in a ".txt" file. All the Figures shown in this chapter have been processed in Matlab. The first measurement is with a hardwall, as is shown in Figure 3.1b. This first measurement acts as a reference for the next ones. In addition, the passive absorbers are measured for a better comparison with the active control.

4.1 Resonance Peaks

4.1.1 Second Resonance

For the first active control measurement, the goal was to diminish the second resonance. In order to make this possible, the quality factor had to reach twice its nominal value.

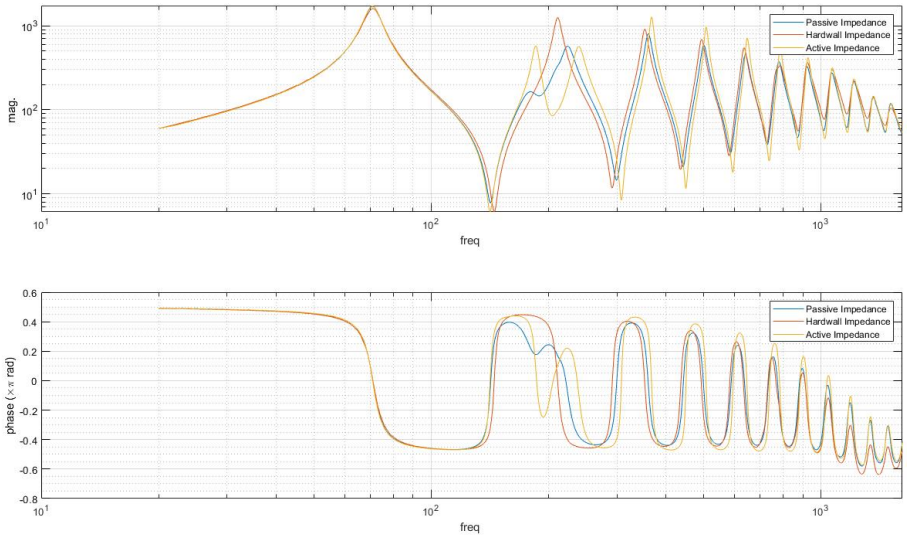

Figure 4.1: $R_{st} = 50[\Omega]; f_t = 250[Hz]; Q_t = 11$

In this measurement, the passive absorption reduces the impedance without controlling the absorbers. The active control reduces the impedance by more than an order of magnitude. On the other hand, it causes two new peaks next to the targeted impedance.

4.1.2 Third Resonance

For the subsequent measurement, the goal was to diminish the third resonance. In order to have a better coherence, the quality factor had to be raised to 20.

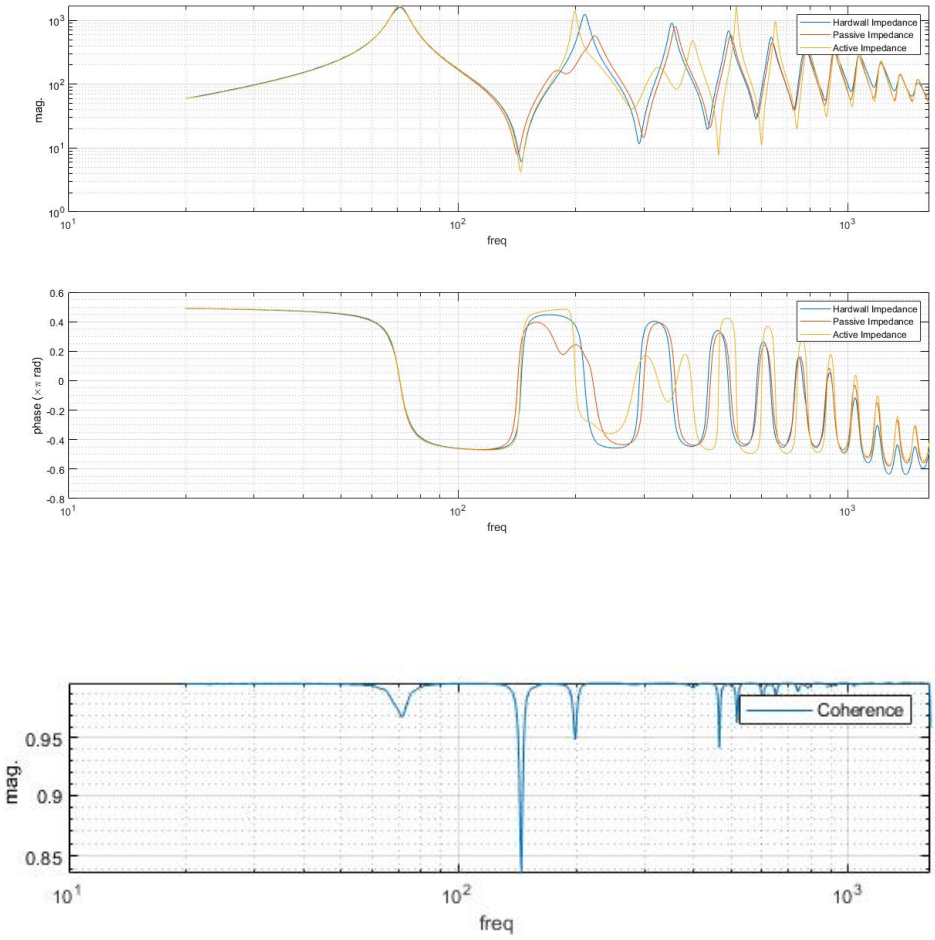

Figure 4.2: $R_{st} = 50[\Omega]; f_t = 420[Hz]; Q_t = 20$

After this measurement, the third resonance was reduced by one order of magnitude, as seen in Figure (4.2). There was a disturbance in the coherence at 150 [Hz], not affecting the targeted frequency. It is noticeable that the other resonance peaks in higher frequencies are more pronounced as a side effect.

4.1.3 Fourth Resonance

The last measurement targets the fourth resonance peak. In order to accomplish this, the quality factor needs to reach high values. The quality factor is directly related to the stability that a system has. The higher the quality factor, the better coherence it has due to the stability of the system. On the other hand, experimentally, the quality factor cannot exceed ten times its mechanical value. A too high quality factor can make the system less and less stable.

It needs to be taken into account that there are four speakers but only one target quality factor. Thus, some of them are exceeding their limits. Two quality factors will be tested for the last measurement, targeting the same frequency. This will show the difference in behaviour between the two quality factors.

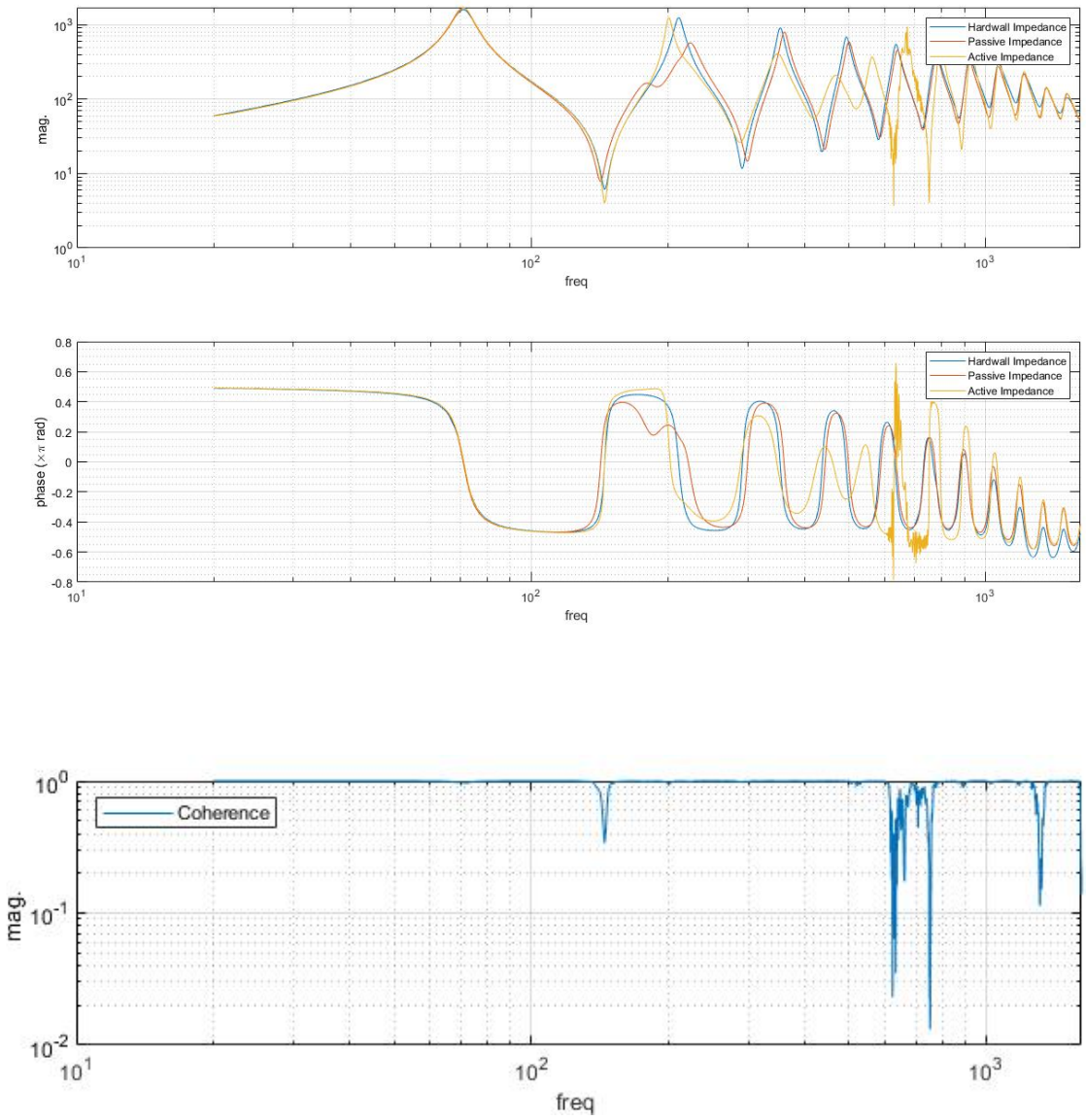

Figure 4.3: $R_{st} = 50[\Omega]; f_t = 600[Hz]; Q_t = 30$

The goal of the measurement was achieved: the fourth resonance was diminished, as shown in Figure (4.3). The drawback is that, as the coherence shows, the measurement has not a linear behaviour after the targeted frequency. This non-linear behaviour can also be seen in the magnitude plot. This could be annoying when heard, as it produces noise in that frequency. Another measurement with a higher quality factor value is done to address this problem.

In this measurement, the quality factor is 50. Compared with the results of the characterization of the speakers, the quality factor is one order of magnitude higher. The targeted frequency is 600 [Hz], as in the last measurement.

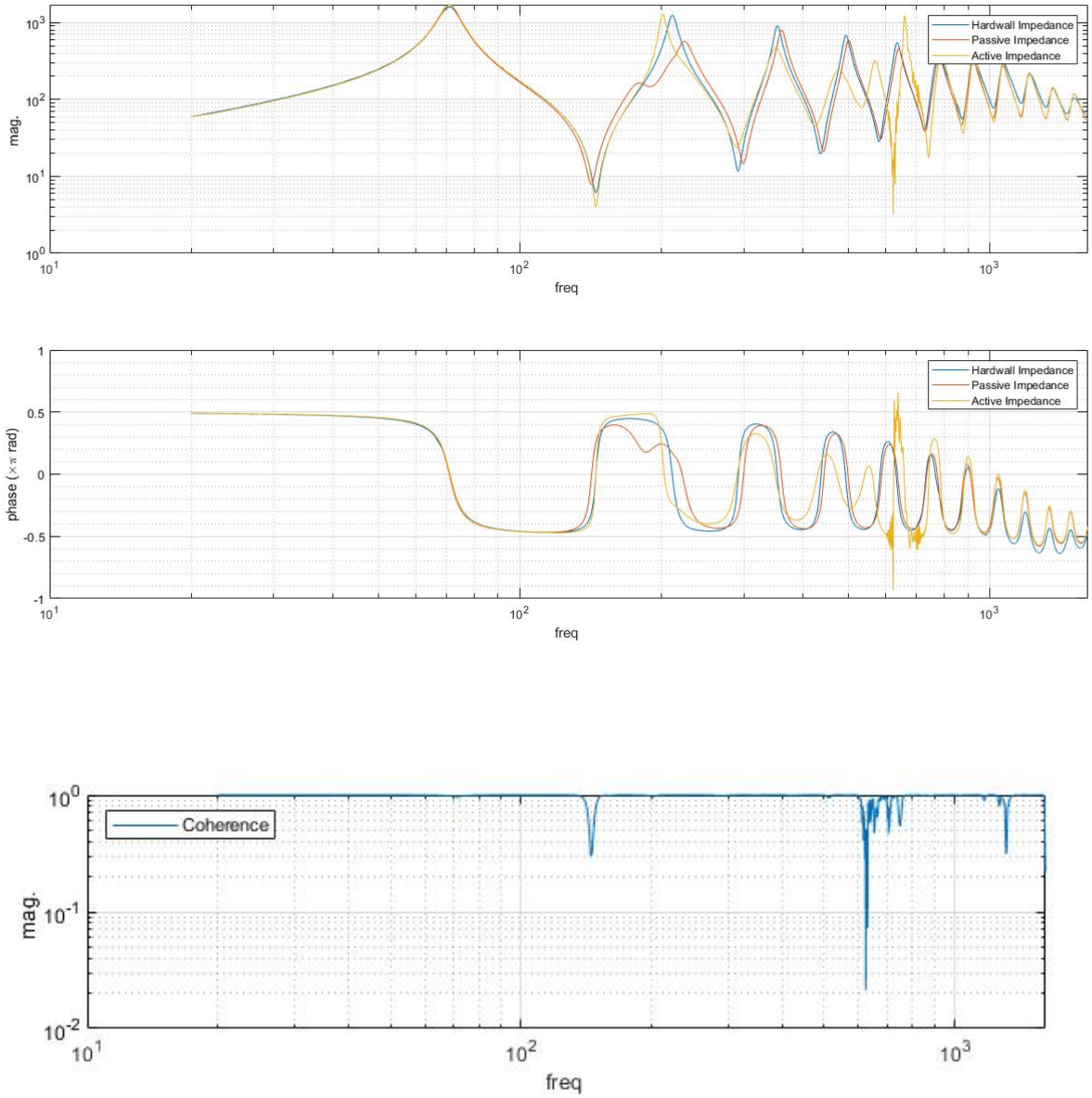

Figure 4.4: $R_{st} = 50[\Omega]; f_t = 600[Hz]; Q_t = 50$

As Figure (4.4) shows, the coherence has improved since last measurement. As a drawback, it is noticeable that the centre of the target frequency has been displaced from before. Therefore, it is not exactly in the fourth resonance but slightly higher. In order to address this phenomenon, the target frequency could be lowered.

4.2 Radiation Impedance

This project aims to change the timbre of an instrument, and this last section intends to show the last piece of the puzzle. In order to judge if the timber has changed, radiation sound measures must be taken. For this to happen, a new setup has to be mounted (Figure 5.4) . A new microphone was located one meter away from the termination on the duct. Now the measurement is between the input pressure and the radiated pressure. Thus, the transfer function between the pressure in these two microphones was taken in the Lapshop software.

4.2.1 Second Resonance

For this section, the hardwall and the passive behaviour of the absorbers had to be measured for comparison. In order to preserve structure among the project, the values remain the same as in the last section. (Figure 4.1)

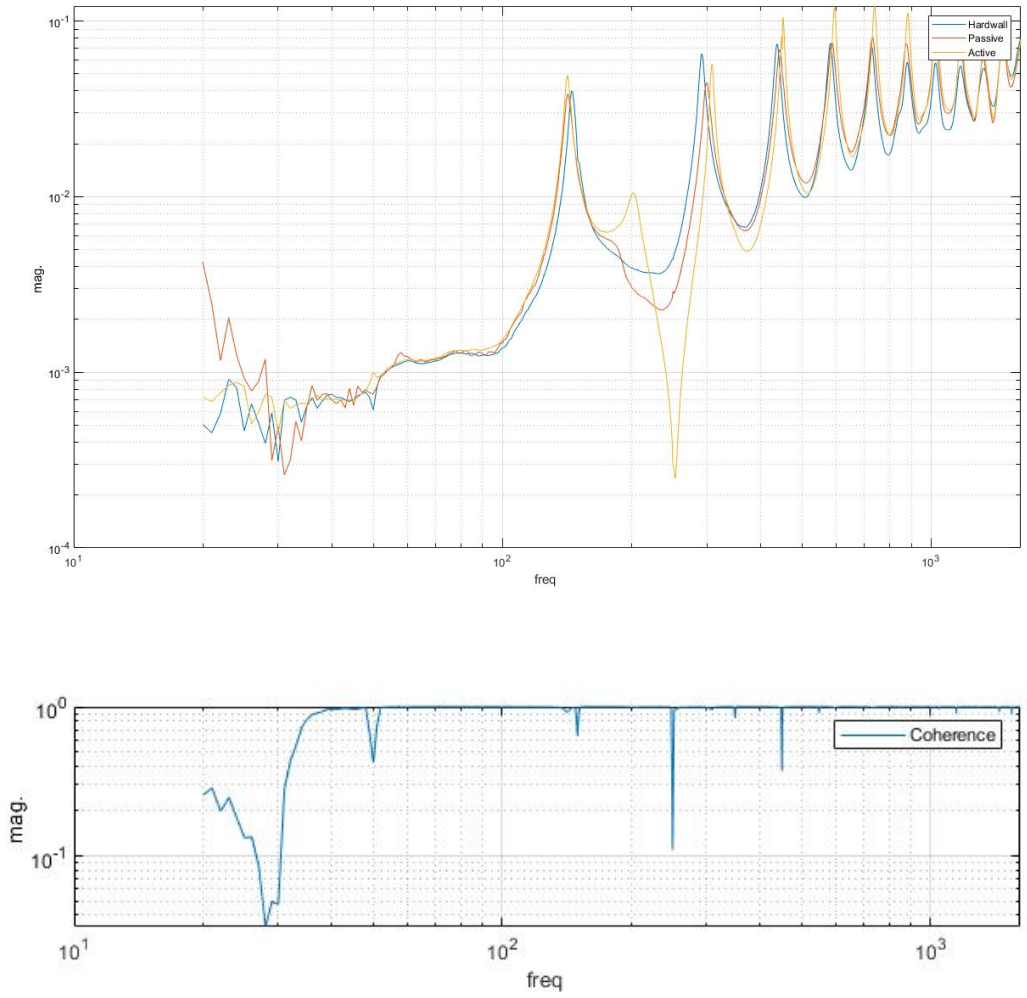

Figure 4.5: Transfer Function between input pressure and radiated pressure; $R_{st} = 50[\Omega]$; $f_t = 250[Hz]$; $Q_t = 11$

Discarding the lower frequencies under 50 [Hz], which have low coherence values, the coherence over the spectrum has a linear behaviour. As it can be seen in Figure (4.5), the peak of resonance outside the duct is in a higher frequency than where the target impedance was supposed to have an effect.

4.2.2 Third Resonance

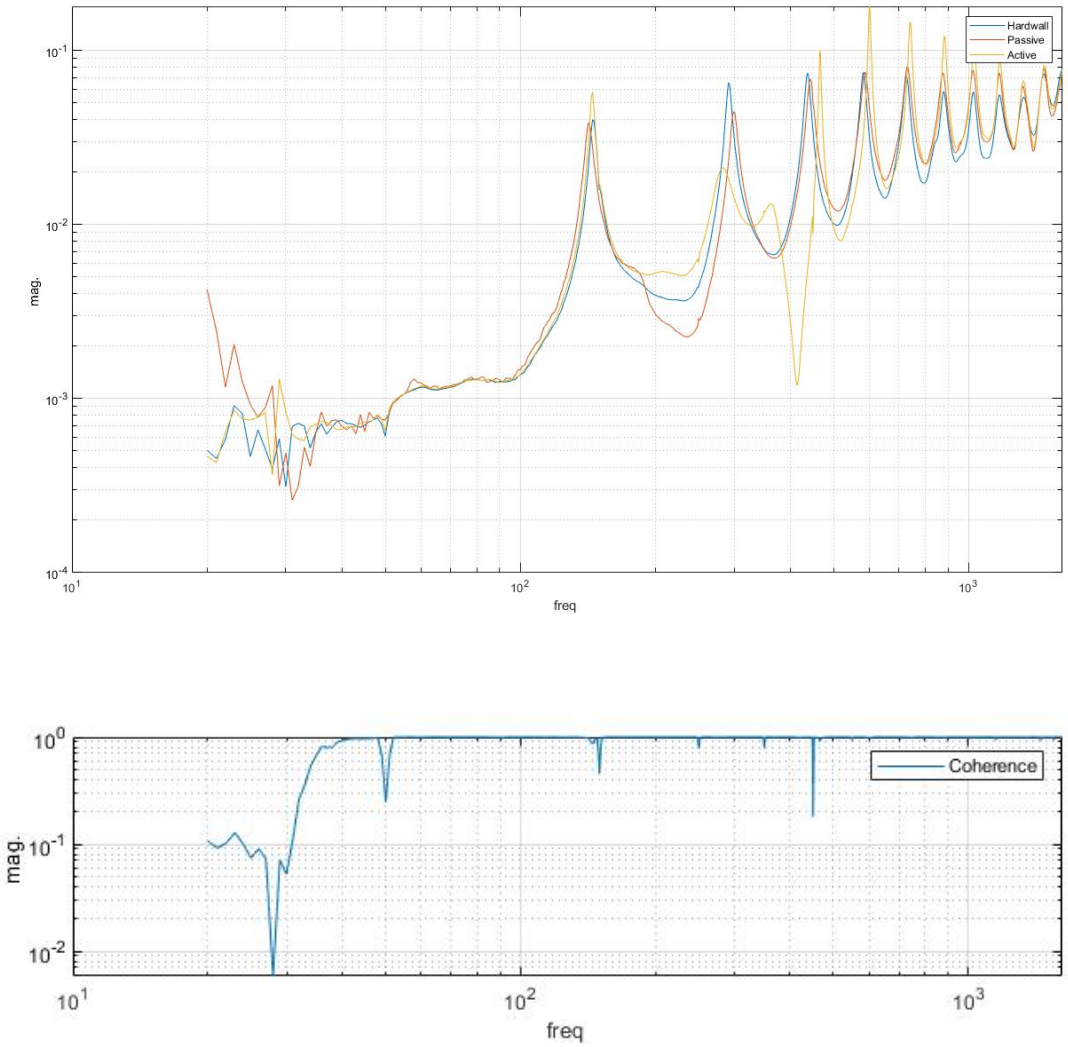

Figure 4.6: Transfer Function between input pressure and radiated pressure; $R_{st} = 50[\Omega]$; $f_t = 420[Hz]$; $Q_t = 20$

In Figure 4.6, the third resonance was target, with successful results. With these settings, the magnitude of the impedance drops almost one order magnitude. If the target frequency had been moved slightly higher, it would have dropped almost two orders of magnitude. It is perceptible that, as before, the targeted frequency is not exactly the peak of the resonance. Furthermore, in this case, the second resonance peak is also diminished by this active control.

For this reason, the following measurement aims too on the third resonance peak, moving the f_t from 420 Hz to 450 Hz.

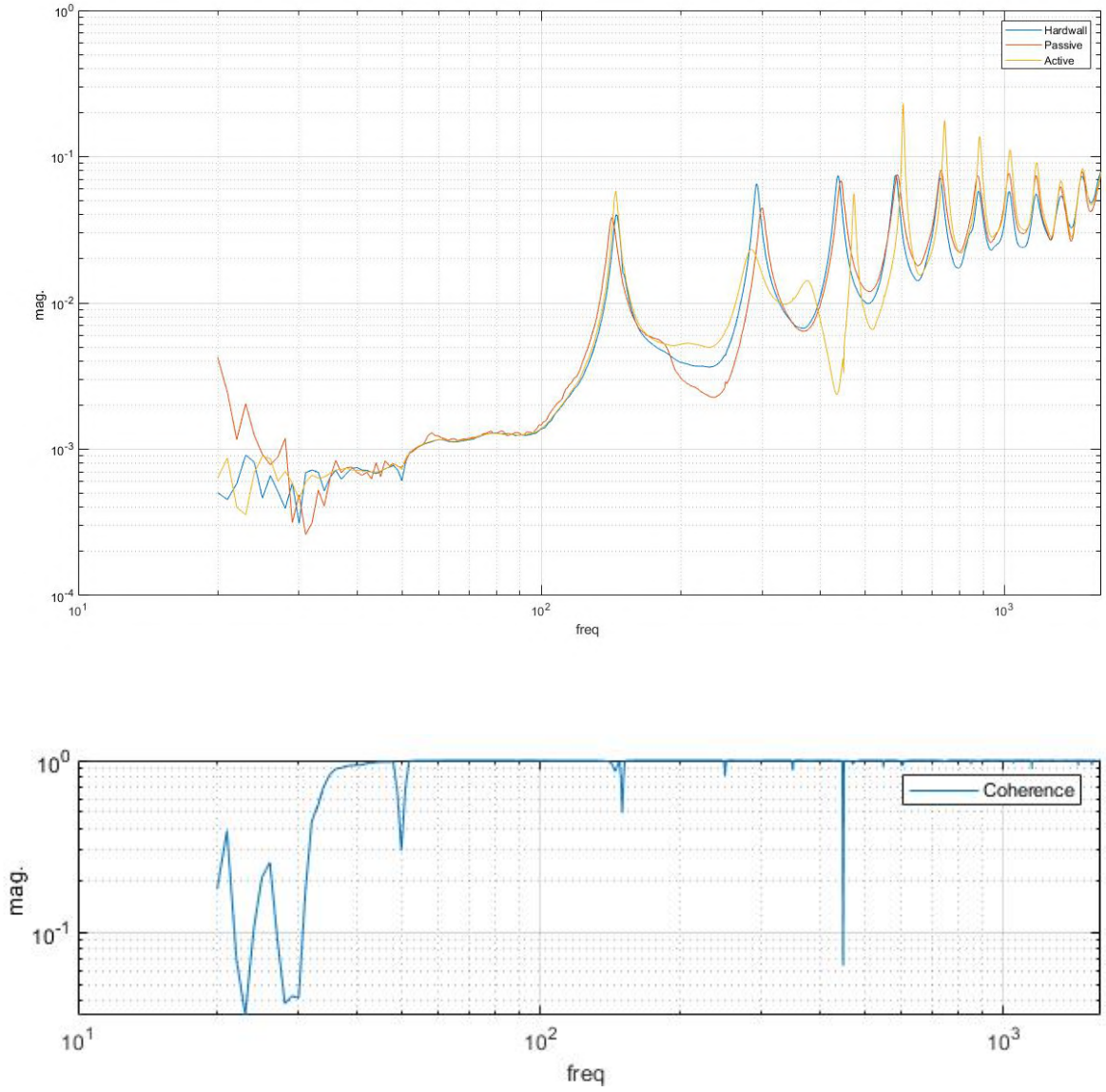

Figure 4.7: Transfer Function between input pressure and radiated pressure; $R_{st} = 50[\Omega]$; $f_t = 450[Hz]$; $Q_t = 20$

As expected, this measurement targets with more accuracy the third resonance. On the other hand, the coherence drops at the targeted frequency. This also raises the magnitude at the peaks of the higher frequencies significantly.

4.3 Limits

During the experimental measures, it is noticed that going lower than 150[Hz] does not produce a fall in the magnitude of the impedance. Moreover, the resistance needs to be lowered when targeting the frequency at lower frequencies.

On the other hand, this could be used in order to enhance certain frequencies in the anti-resonances.

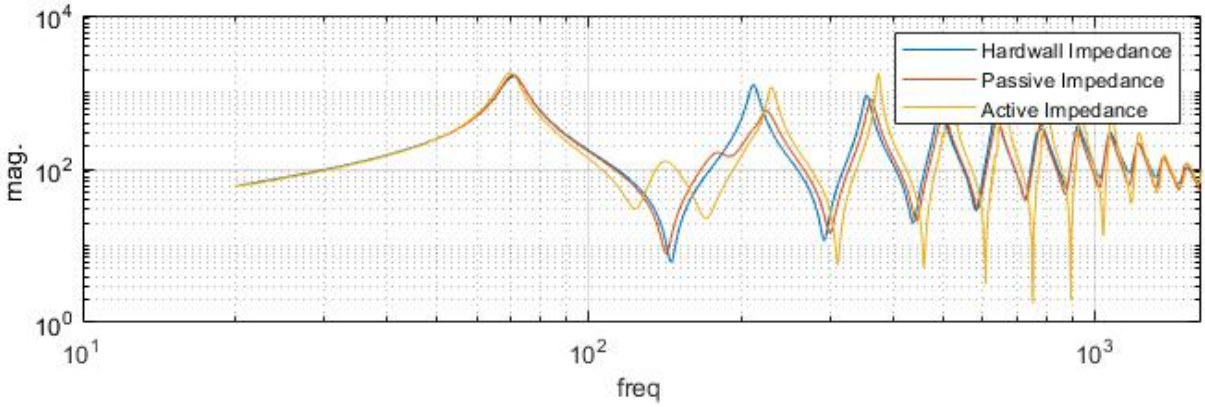

Figure 4.8: Active control. $R_{st} = 50[\Omega]$; $f_t = 200[Hz]$; $Q_t = 8$

In Figure (4.8) it is shown how an active control of the parameters at 200Hz produces an enhance of the magnitude at the anti-resonance between the first two resonances of the duct.

4.4 Conclusion

The project's goal was to control the acoustic impedance and alter the timbre of the duct. As this report shows, this is feasible with the right equipment and precise control over it. The main limitation is the flexibility of the parameters of the speaker, which only allows us to control the timbre over a small range of low-mid frequencies in this exercise. Possible issues include unexpected new resonances and noise that is due to the control operating near its stability limits.
Controlling the timber is not merely to diminish the impedance of the resonances. It could also be understood as boosting the impedance in the anti-resonances enhancing specific frequencies, as seen in Figure (4.8). In this figure, the frequency in 150[Hz] is being enhanced.

Further work would be exploring different sizes of duct and speakers and targeting not only one frequency but more at the same time.

5 Appendix

5.0.1 Matlab & Simulink

For the measurements, Matlab used was to compute and control the values of the electroacoustic absorbers. The use of Simulink facilitates modelling the system to control the electroacoustic absorbers. In order to define the transfer function θ (eq. 2.6), an implementation of a discrete filter for each absorber is needed. Each filter implements the Direct form II to control the coefficients of θ, using the minimal number of delay elements.

In the system, each absorber can be used independently for the calculus of its parameters. The block parameter $[u]$ in Figure 5.1 stands for the input, which represents the analogue microphone. The variables $[y1]$, $[y2]$, $[y3]$ and $[y4]$ represent the outputs.

The function **get_parameter()** has a theta (θ) set by default. This function retrieves the three parameters from the impedance and then provides the pressure factor. It also rectifies the velocity of the membrane measured from the side with a correction factor.

When using the function **set_target()**, in order to actively control the impedance, the parameters must be changed manually. Otherwise, it has a default *theta*. When the targeted parameters f_s, Q_{ms} and R_{ss} are manually set, the transfer function theta is converted from continuous to discrete. Then, it computes the transfer function coefficients that the system will later use.

To assess the states (On/Off) of the absorbers, the function **set_state()** provides the ability to enable, independently or synchronously, the absorbers. In *Simulink*, this is represented with a Switch.

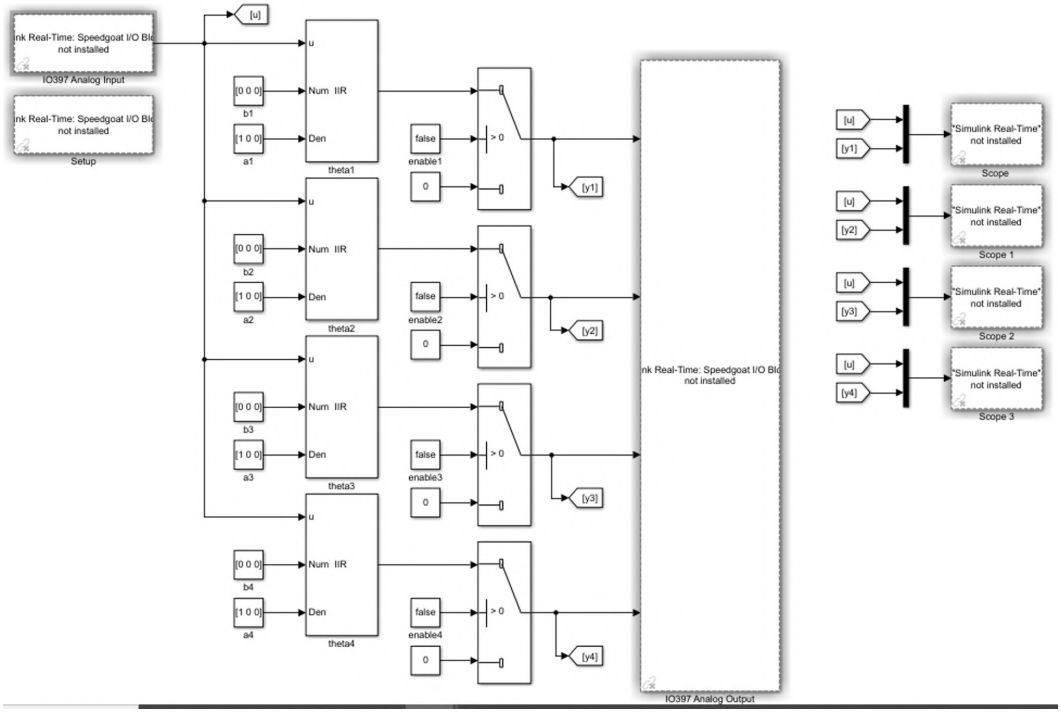

Figure 5.1: Simulink

The impedance Z_s is known from a passive measurement and another when using a known theta. This provides the ability to retrieve the force factor with a transfer function between both measurements.

5.1 Equipment

Other equipment used in the measurements included is shown in Figure (5.2). The figure shows:

- 1.Converter 10mA/V.
  This was used to connect the current received from the controller "Speedgoat" to the four speakers. For its proper functioning, it had to be connected to an amplifier that can be glimpsed in the middle left part of the image.

- 2.Output/Input.
  This device was used to connect the pressure from the microphone in the absorbers to the Brüel Kjær Type 3160-A-042 Output Generator Module 50kH.

- 3. Polytec OFV-5000 VIBROMETER CONTROLLER.
  This is the laser that controls the velocity of the diaphragm of the absorbers and source speaker.

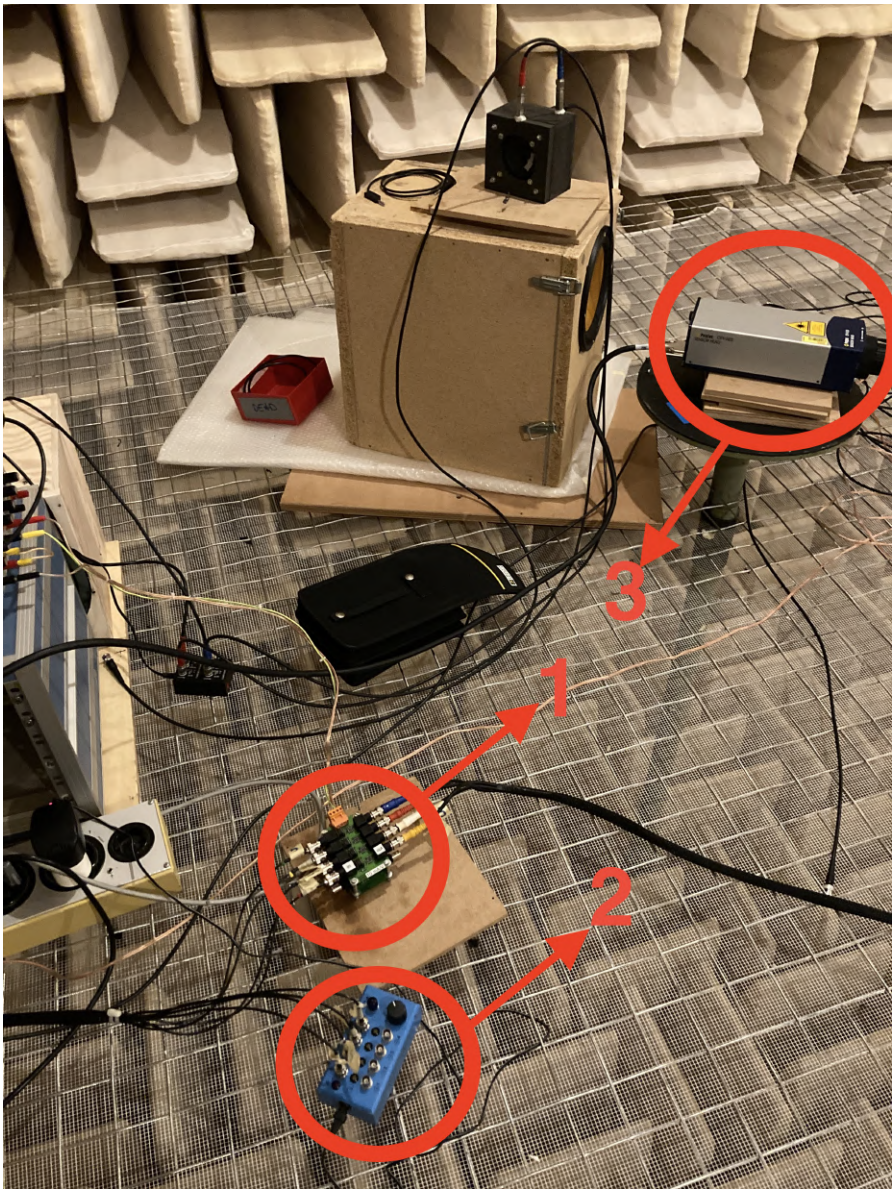

Figure 5.2: 1.Conversor 10mA/V ; 2.Output/Input ; 3. Vibrometer

This image (Figure 5.3) shows the control and measurement of the absorbers with the vibrometer focalizing in the diaphragm of one of them. Here, the reflective tape is visible to improve the reflection of the vibrometer. This image was taken during the characterization of the absorbers.

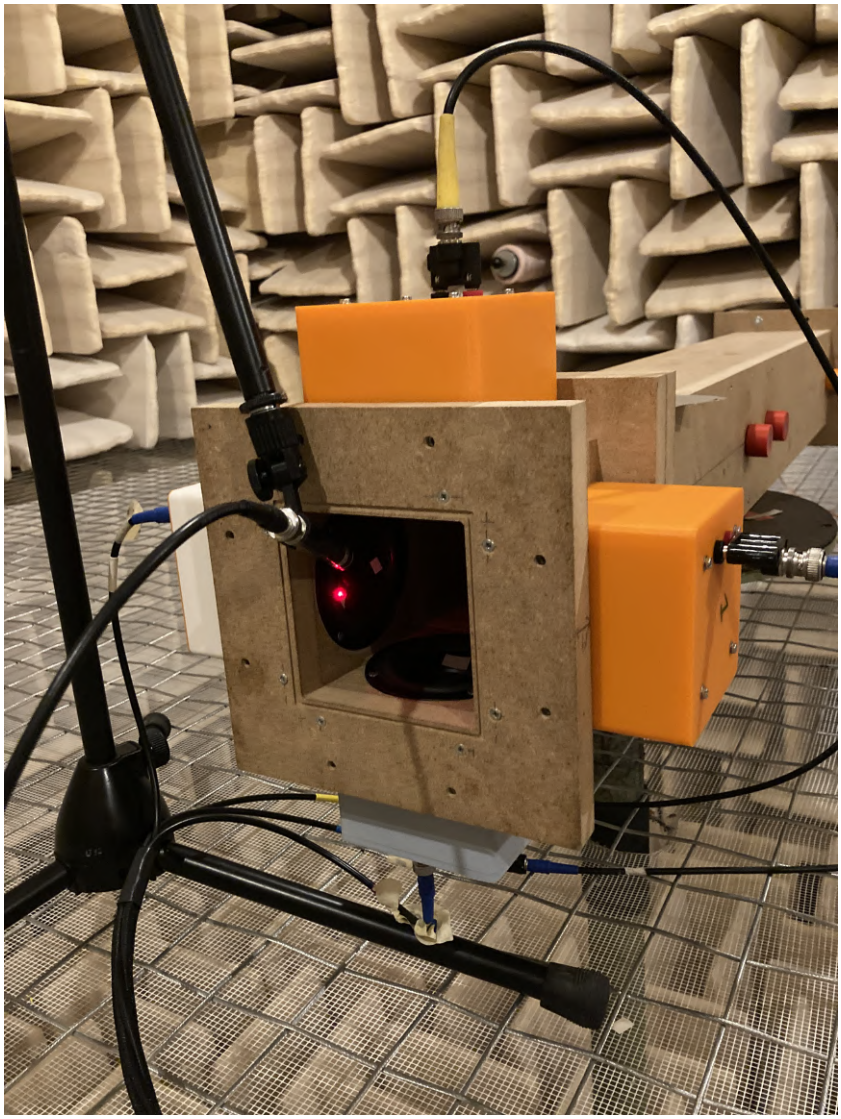

Figure 5.3: Characterization of the absorbers.

Moreover, in this image (figure 5.4) it is shown the last setup, with a third microphone at 1 meter from the termination of the duct, in order to measure the ratio between the pressure on the source and the pressure 1 meter ahead of the duct opening.

Figure 5.4: Radiation Impedance Setup

This is done because in the simulation, there is a pressure source of 1 [Pa] and the pressure outside the duct is simulated one meter ahead of the opening of the duct.

To compare the measurement to the simulation, since there is not an ideal pressure source in the physical world, it ought to be compared to the pressure at the source. The latter is done with a microphone. The other microphone in the absorbers is only used for controlling the absorbers.

Bibliography

[1] WOLFE, Joe; CHEN, Jer-Ming; SMITH, John. The acoustics of wind instruments–and of the musicians who play them. En Proceedings of the 20th International Congress on Acoustics, ICA-2010. 2010.

[2] RIVET, Etienne Thierry Jean-Luc. Room modal equalisation with electroacoustic absorbers. EPFL, 2016.

[3] TAILLARD, P.-A., et al. Modal analysis of the input impedance of wind instruments. Application to the sound synthesis of a clarinet. Applied acoustics, 2018, vol. 141, p. 271-280.

[4] SILVA, Fabrice, et al. Approximation formulae for the acoustic radiation impedance of a cylindrical pipe. Journal of Sound and Vibration, 2009, vol. 322, no 1-2, p. 255-263.

[5] LISSEK, Hervé; BOULANDET, Romain; FLEURY, Romain. Electroacoustic absorbers: bridging the gap between shunt loudspeakers and active sound absorption. The Journal of the Acoustical Society of America, 2011, vol. 129, no 5, p. 2968-2978.

[6] CHAIGNE, Antoine; KERGOMARD, Jean. Acoustique des instruments de musique. Belin, 2008.

[7] ROSSI, Mario. Audio. PPUR presses polytechniques, 2007.

[8] Theo2 (2022). Struve functions.(https://www.mathworks.com/matlabcentral/fileexchange/37302-struve-functions) MATLAB Central File Exchange. Retrieved June2, 2022.

[9] https://github.com/EduardoJoseGonzalezColl/SemesterProject

[10] DALMONT, J.-P. Acoustic impedance measurement, Part I: A review. Journal of Sound and Vibration, 2001, vol. 243, no 3, p. 427-439.

[11] FÉLIX, Simon; DALMONT, Jean-Pierre; NEDERVEEN, C. J. Effects of bending portions of the air column on the acoustical resonances of a wind instrument. The Journal of the Acoustical Society of America, 2012, vol. 131, no 5, p. 4164-4172.

[12] EVENO, Pauline. L'impédance d'entrée pour l'aide à la facture des instruments de musique à vent: mesures, modèles et lien avec les fréquences de jeu. 2012. Tesis Doctoral. Université Pierre et Marie Curie-Paris VI.

[13] XIN, Bo, et al. Experimental and numerical investigation of anechoic termination for a duct with mean flow. Applied Acoustics, 2018, vol. 139, p. 213-221.

[14] RICHARDSON, Mark H.; FORMENTI, David L. Global curve fitting of frequency response measurements using the rational fraction polynomial method. Proceeding of 3rd IMAC, 1985, p. 390-397.